Ultrasonic Motors With Polymer-Based Vibrators

Jiang Wu, Yosuke Mizuno, *Member, IEEE*, Marie Tabaru, and Kentaro Nakamura, *Member, IEEE*

***Abstract*—With their characteristics of low density and elastic moduli, polymers are promising materials for making ultrasonic motors (USMs) with high energy density. Although it has been believed for a long time that polymers are too lossy to be applied to high-amplitude vibrators, there are several new polymers that exhibit excellent vibration characteristics. First, we measure the damping coefficients of some functional polymers to explore the applicability of polymers as vibrators for USMs. Second, to investigate the vibration characteristics, we fabricate bimorph vibrators using several kinds of polymers that have low attenuation. Third, a bending mode USM is fabricated with a polymer rod and four piezoelectric plates bonded on the rod as a typical example of a USM. Through an experimental investigation of the motor performance, it was found that the polymer-based USMs exhibited higher rotation velocity than the aluminum-based USM under a light preload, although the maximum torque of the polymer-based USMs was smaller than the aluminum-based USM. Among the tested polymers, polyphenylenesulfide was a prospective material for USMs under light preloads because of the high amplitude and lightweight of polyphenylenesulfide.**

I. Introduction

With their characteristics of low speed, high torque, and quick response [1], ultrasonic motors (USM) have been applied in robots, precision positioning machines, and optical instruments. As an important part of a mechanical system, an actuator with high energy density can decrease the total weight of the system and increase the operability. Many researchers have focused on developing micro-sized USMs [2]–[10], whose vibrators were made primarily of metal or piezoelectric ceramics [11]. MEMS technology is also used to miniaturize USMs; however, this is applicable only to micro motors smaller than 1 mm, and available materials are limited. On the other hand, reducing the weight of actuators is another important issue. A variety of new functional polymers have been invented in the last 30 years with the development of material science, and some of the polymers have good workability and wear characteristics [12]. In some of the previous reports on USMs, polymer film was glued to the contacting surface as a friction material to improve the friction and wear characteristics [13]–[16]. However, polymers have never been used as the vibrating body of a USM. To reduce weight, it would be meaningful to examine the possibility of applying polymers as both the vibrator and rotor of a USM.

Polymers usually appear to be very soft and good for absorbing vibration as a result of high mechanical loss. However, among new kinds of engineering polymers, some products with low mechanical loss exist. To gain a preliminary understanding of the attenuation characteristics of the polymers, we measured the damping coefficients of some typical functional polymers: polyetheretherketone (PEEK), polyacetal (POM), acrylonitrile-butadiene-styrene (ABS), polyphenylenesulfide (PPS), and polyphenylenesulfide filled with carbon fiber (PPS/CF). Next, we selected the polymers with low damping coefficients to fabricate bar-type USMs and investigated the vibration and mechanical characteristics of those USMs.

II. Polymer-Based Bimorphs

A. Introduction of the Tested Polymers

Since the first report about its excellent mechanical properties, PEEK has been a promising substitute material for metal. At present, the current version of PEEK has excellent abrasion resistance and workability [12], [17]. In industrial applications, lightweight gears are often made of POM because of its high resistance to abrasion and heat [18]. ABS has flowability and high resistance to impact [19]. PPS is also widely applied in the automotive industry because it has better wear properties than PEEK [20]. To increase strength, other materials such as glass, carbon fiber, and aramid fiber are filled in bars or plates of PPS. The composite, using carbon fiber as filler component with a mass fraction of 30%, is referred to as PPS/CF. The carbon fibers are filled in parallel in one direction; thus, this composite has obvious anisotropy. The mechanical characteristics of PEEK, POM, ABS, PPS, and PPS/CF used in the experiments in this paper are listed in Table I. Note that the elastic modulus of the PPS/CF shown in Table I is the value in the direction of the carbon fibers.

B. Preliminary Measurement of the Damping Coefficients

Because the attenuation characteristics for the kilohertz vibration of the polymers used in the experiments have rarely been reported, we measure the damping coefficients of these functional polymers before conducting our

Manuscript received April 17, 2015; accepted October 1, 2015. The authors thank Daicel Corporation for providing some of the polymer samples tested in the experiments.

The authors are with the Precision and Intelligence Laboratory, Tokyo Institute of Technology, Yokohama 226-8503, Japan (e-mail: wujiang@sonic.pi.titech.ac.jp).

DOI http://dx.doi.org/10.1109/TUFFC.2015.007122

TABLE I. MECHANICAL CHARACTERISTICS OF THE TESTED POLYMERS AND ALUMINUM.

Material	Density ($\times 10^3$ kg/m^3)	Elastic modulus (GPa)	Poisson's ratio
PEEK	1.28	3.5	0.40
POM	1.41	2.8	0.35
ABS	1.05	2.4	0.36
PPS	1.35	3.45	0.36
PPS/CF	1.44	21.2*	—
Aluminum	2.70	70.3	0.33

*Measured in filling direction.

experiments to make preliminary choice of the polymers suitable for vibrators. As a comparison, the damping coefficient of aluminum is also measured.

Fig. 1 shows the experimental setup. One end of the bar of 100 mm in length, 10 mm in width, and 1.5 mm in thickness was fixed to an acrylic base using a bolt. We hammered the middle of the bar to give it a transient mechanical input, and measured the vibration velocity at the free end using a laser Doppler velocimeter (NLV1232, Polytec, Waldbronn, Germany). A damped oscillation of the velocity $v(t)$ with an exponential envelope, as shown in Fig. 2, is theoretically expected. The vibration velocity $v(t)$ is given by the equation

$$v(t) = V_0 \cdot e^{-\beta\omega_0 t} \cdot \sin(\omega_0 t + \theta), \quad (1)$$

where V_0, 2β, ω_0, and θ are the initial velocity amplitude, the damping coefficient, the resonance frequency, and the phase. We calculated the damping coefficients 2β by fitting the measured data with the envelope of (1). The measurements were carried out 20 times for each sample, and the averaged value was selected as the damping coefficient of the sample.

Fig. 3 shows the results. The damping coefficient of PPS is 0.003, which is the smallest among the tested polymers. The damping coefficient of PPS/CF increases to 0.006 with the carbon fiber filled into the base-material PPS. The damping coefficients of POM and ABS are eight times larger than that of the PPS. The damping coefficient of aluminum is 0.0005, which is 0.17 times that of PPS. From these results, we decided to use PEEK, PPS, and PPS/CF as the elastomers of bimorphs to test their capabilities as piezoelectric vibrators.

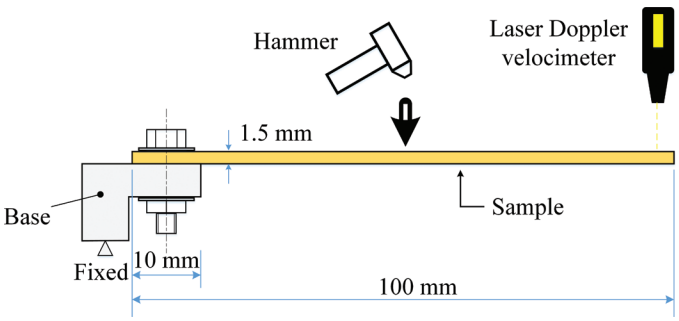

Fig. 1. The experimental setup of the measurement of the damping coefficient.

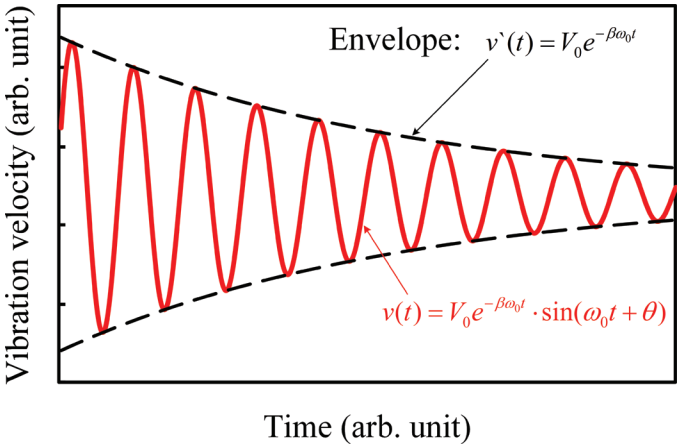

Fig. 2. The theoretical output and envelope curve of vibration velocity in the time domain under a transient input.

C. Structure and Dimensions of the Bimorph

As shown in Fig. 4, two pieces of piezoelectric ceramic plates with a folded electrode (C213, Fuji Ceramics, Fujinomiya, Japan) of 10 mm in length, 4 mm in width, and 0.5 mm in thickness are glued to the side surfaces of a polymer rectangular cantilever using epoxy. The electrical connection of the electrodes to the power source is shown in Fig. 4. When an alternating voltage at the resonance frequency was exerted, a bending mode appeared on the vibrator, although the tested polymers were nonconductive. It should be noted that, for the PPS/CF-based bimorph, the direction of the vibration velocity was approximately vertical to the filling direction of the carbon fibers. The vibration distribution was measured using a laser Doppler velocimeter (NLV1232, Polytec). To compare the performances, bimorphs using PEEK, PPS, and PPS/CF were made with the same dimensions. Meanwhile, a bimorph made of aluminum with the same structure and dimensions was made as a reference. The admittance characteristics were measured using an impedance analyzer (4294A, Agilent, Santa Clara, CA, USA), and the results of the PEEK-, PPS-, PPS/CF-, and aluminum-based bi-

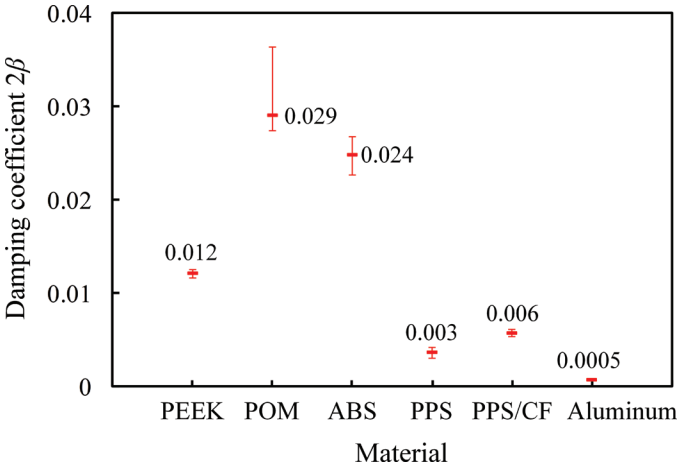

Fig. 3. The measurement results of the damping coefficients.

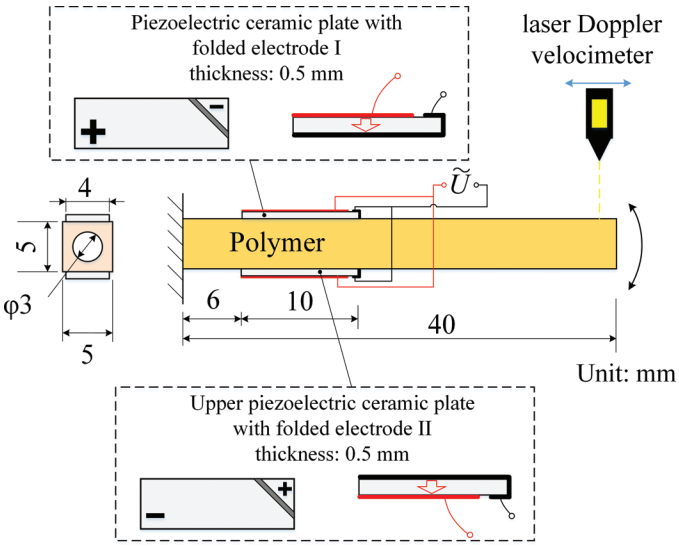

Fig. 4. Structure and dimensions of the bimorph vibrators.

morphs are demonstrated in Figs. 5(a)–5(d), respectively. Electrical responses corresponding to the 1st, 2nd, and 3rd bending modes are observed in the admittances. The 3rd bending mode shows the most obvious response because the position of the piezoelectric ceramic is near the antinode of the 3rd mode.

To precisely obtain the mechanical quality factors (Q factors) of the bimorphs, we measured the frequency response of the vibration velocity at the free end of the vibrator around the resonance frequency of the bending modes. The Q factors are calculated according to the approximate equation

$$Q = \frac{f_0}{\Delta f}, \tag{2}$$

where f_0 and Δf represent the resonance frequency and the bandwidth for $1/\sqrt{2}$ of the amplitude, respectively.

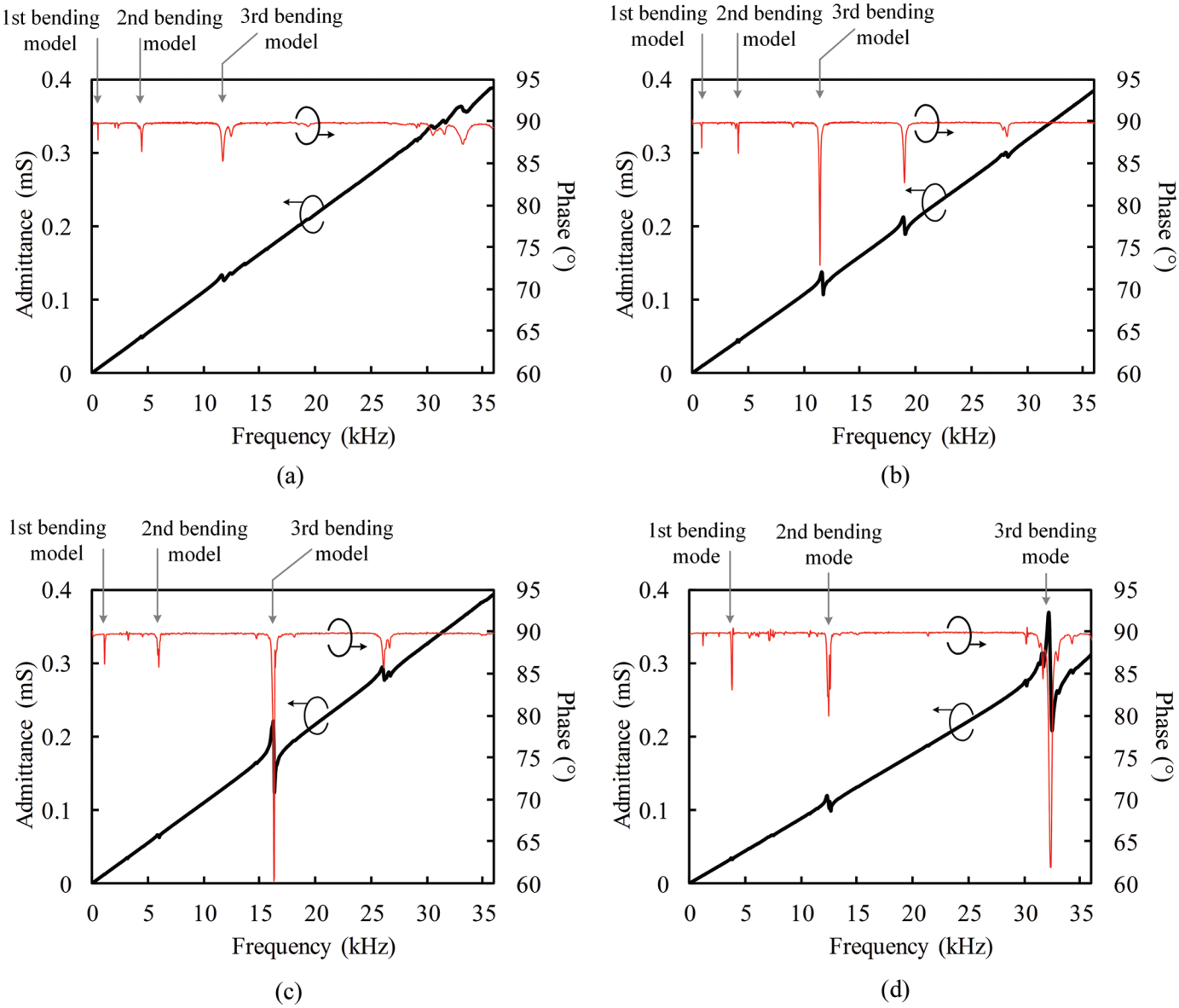

Fig. 5. Admittance characteristics of (a) PEEK-, (b) PPS-, (c) PPS/CF-, and (d) aluminum-based bimorph vibrators.

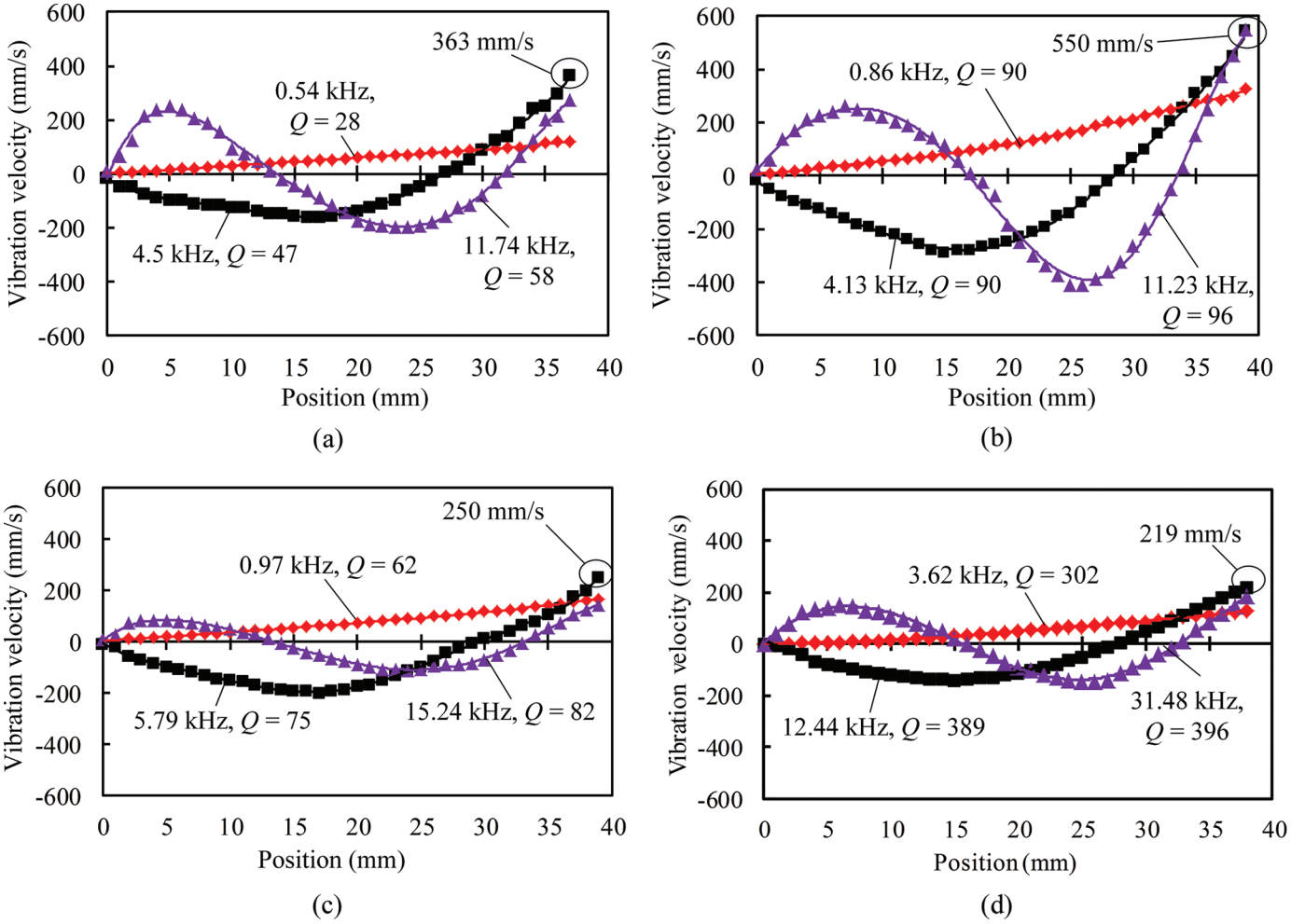

Fig. 6. Vibration velocity distribution of (a) PEEK-, (b) PPS-, (c) PPS/CF-, and (d) aluminum-based bimorph vibrators for the 1st, 2nd, and 3rd bending modes at the driving voltage of 60 V.

D. Results

The vibration velocities were measured along the bar at an interval of 1 mm at a driving voltage of 60 V. Figs. 6(a)–6(d) show the results with Q factors for the PEEK-, PPS-, PPS/CF-, and aluminum-based bimorphs. The PEEK vibrator had its natural frequencies of the 1st, 2nd, and 3rd bending modes at 0.54, 4.5, and 11.74 kHz, respectively, and the maximum vibration velocity reached 363 mm/s at the free end. The resonance frequencies of the 1st, 2nd, and 3rd bending modes for the PPS vibrators were 0.54, 4.13, and 11.23 kHz, respectively. The maximum vibration velocity was 550 mm/s at the 3rd bending mode. The natural frequency of each mode increased for the PPS/CF vibrator, exhibiting higher values of 0.97, 5.79, and 15.24 kHz; meanwhile, the maximum vibration velocity fell to 250 mm/s at a driving frequency of 5.79 kHz. The Q factors of the PPS- and PPS/CF-based bimorphs were higher than those of the PEEK-based bimorph. For the aluminum-based vibrator, the natural frequencies of 1st, 2nd, and 3rd bending modes were 3.62, 12.44, and 31.48 kHz, respectively. The maximum vibration velocity reached 219 mm/s at a driving frequency of 12.44 kHz. The Q factors of the aluminum-based vibrators were higher than those of the polymer-based vibrators. For comparison, the resonance frequency, the Q factor, and the maximum vibration velocity of the 2nd bending mode are summarized in Table II. It is clear that the resonance frequency of the aluminum-based bimorph is three times that of the polymer-based ones, and the resonance frequencies of the PEEK- and PPS-based bimorphs exhibit little difference. The vibration velocities of the polymer-based bimorphs are larger than that of the aluminum-based bimorph. Among polymer-based bimorphs, the maximum vibration velocity of the PPS-based bimorph reaches 543 mm/s, which is larger than that of the others.

TABLE II. VIBRATION PERFORMANCES OF POLYMER-BASED AND ALUMINUM-BASED BIMORPH VIBRATORS OF THE 2ND BENDING MODE.

Elastomer	Resonance frequency (kHz)	Q factor	Maximum vibration velocity (mm/s)
PEEK	4.50	47	363
PPS	4.13	90	543
PPS/CF	5.79	75	250
Aluminum	12.44	389	219

E. Discussion

To discuss the relationship between the performance (resonance frequency and vibration velocity) and the mechanical parameters, an electrical equivalent circuit model shown in Fig. 7 is introduced [3], [5], [21]. Coefficient A represents the transformation ratio from voltage V to driving force F, whereas m, k, and μ represent the equivalent mass, bending stiffness, and mechanical resistance of the 2nd bending model, respectively. Vibration velocity v is simulated by the current in the circuit. Resonance frequency f is determined by the equivalent mass m and bending stiffness k:

$$f = \frac{1}{2\pi}\sqrt{\frac{k}{m}}. \tag{3}$$

Bending stiffness k is closely related to elastic modulus E, whereas equivalent mass m is proportional to density ρ. Thus, the resonance frequency is proportional to a square root of the elastic modulus and inversely proportional to a square root of the density if the vibration mode is specified. According to [22], the resonance frequency of the 2nd bending mode of the clamped-free bimorph is given as

$$f = \frac{1}{2\pi}\cdot\left(\frac{4.694}{l}\right)^2\sqrt{\frac{EI}{\rho S}}, \tag{4}$$

where l, I, and S represent the length, the area moment of inertia, and the cross-sectional area of the cantilever, respectively. Although the resonance frequency is determined by the ratio of the elastic modulus to the density, the lower resonance frequency of the polymer-based bimorph compared with the aluminum-based bimorph is mainly attributed to the lower elastic modulus. This is because the ratio of aluminum to PPS in the elastic modulus is much larger than that of the density. The PEEK- and PPS-based vibrators show little difference in their resonance frequencies because their elastic moduli and densities are almost the same. According to (4), the effective elastic modulus of PPS/CF in the bending mode is lower than 21.2 GPa.

Next, we carry out an analysis of the relationship between the vibration velocity and the mechanical parameters. Based on the circuit shown in Fig. 7, under the resonant state, the vibration velocity is

$$v = \frac{VA}{\mu}. \tag{5}$$

In a mechanical resonance system, the mechanical resistance μ can be expressed with the mechanical quality factor Q, the equivalent mass m, and the bending stiffness k of the vibrator [21]:

$$\mu = \frac{\sqrt{k\cdot m}}{Q}. \tag{6}$$

Substituting (6) into (5), we obtain

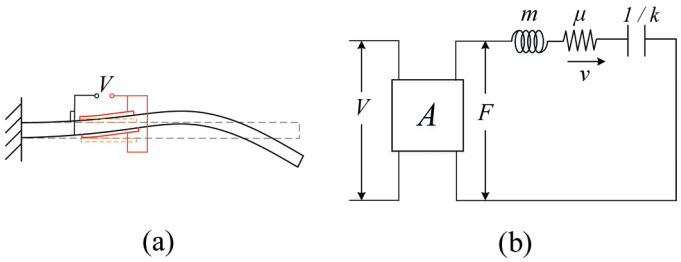

Fig. 7. Electrical equivalent circuit representing the vibration characteristics of the 2nd bending mode. (a) The bimorph vibrator in the 2nd bending mode, (b) electrical equivalent circuit.

$$v = VA\cdot\frac{Q}{\sqrt{k\cdot m}}. \tag{7}$$

Because the bending stiffness is related to the elastic modulus, and the equivalent mass is determined by the density, vibration velocity v is proportional to the Q factor, and inversely proportional to the square root of the product of elastic modulus E and density ρ. First, let us compare the vibration velocity of the polymer-based vibrator with that of the aluminum-based vibrator. The polymer-based vibrators exhibit higher vibration velocities than the aluminum vibrator as summarized in Table II. This is attributed mainly to the extremely low elastic modulus of the polymers compared with that of the aluminum. Second, the difference in the vibration velocities of the PEEK- and the PPS-based vibrators mainly originates in the difference in the Q factors because the elastic moduli and densities are almost the same.

To summarize, we draw the following conclusions for the bimorph vibrators made of different materials under certain dimensions:

1) Resonance frequency of the polymer-based bimorph is lower than the aluminum-based one with the same dimensions because of a lower elastic modulus.
2) Vibration velocity of the polymer-based bimorph is higher than that of the aluminum-based one because of a lower elastic modulus.
3) PPS-based bimorph has a higher vibration velocity than other polymer-based ones because of its high Q factor.

III. Standing Wave USM With Two Orthogonal Bending Modes

A. Experimental System

The structure of the polymer-based USM for our experiments is depicted in Fig. 8(a). Four pieces of piezoelectric ceramic plates (10 mm × 6 mm × 0.5 mm) are bonded on the four surfaces of a rectangular bar made of polymer. The length and width of the bar are 44 mm and 6.2 mm, respectively. The end has a disk shape of 8 mm in

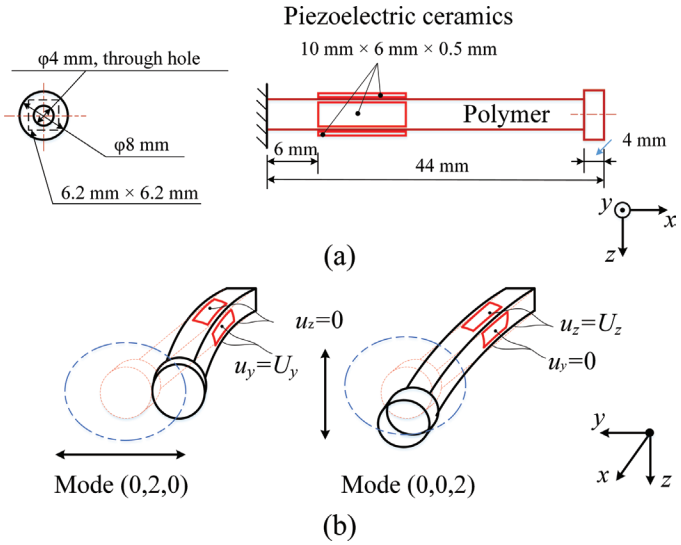

Fig. 8. Dimensions and principle of the polymer-based ultrasonic motor with rectangular bar shape. (a) Structure and dimensions of the vibrator, (b) formation of the elliptical motion with the phase drive of two orthogonal vibrations.

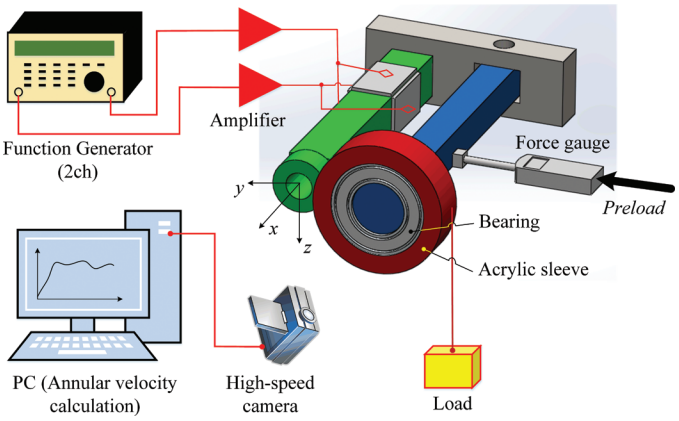

Fig. 9. Experimental setup to evaluate the mechanical characteristics.

diameter and 4 mm in thickness for contact with a rotor. The piezoelectric elements are grouped into two parallel pairs. Two orthogonal bending vibrations are excited with a 90-degree phase difference, with phased voltages applied to the two pairs of the piezoelectric ceramics. The free end of the bar shows an elliptical motion at the driving frequency. A rotor pressed on the free end is driven by the elliptical orbit, as illustrated in Fig. 8(b). The weights of the PEEK-, PPS-, and PPS/CF-based vibrators are 2.649, 2.709, and 2.844 g, respectively. The rotor is composed of an acrylic sleeve and is supported with an aluminum bar via a ball bearing. The total weight of the rotor and the bar is 3.525 g. The experimental system depicted in Fig. 9 is used to measure the mechanical characteristics of the motor. A high-speed camera (M5, Integrated Design Tools Inc., Tallahassee, FL, USA) is used to record the angular position of a marker pasted on the rotor. The angular velocity of the rotor is calculated from the pictures taken with the camera by counting the number of turns of the rotor and the time interval. A force gauge [ZP(Z2)-50N, Imada Co. Ltd., Toyohashi, Japan] is used to simultaneously measure the preload exerted between the vibrator side and the rotor. Output torque is measured by pulling up a weight.

B. Results

First, we measured the angular velocities of the rotor without load under different preloads. The driving frequency was adjusted to obtain the maximum velocity as the preload was varied. The experimental results for the angular velocity and driving frequency are shown in Fig. 10.

The angular velocities of the PPS- and PPS/CF-based USMs were over 30 rad/s, and fell sharply after the preload exceeded 800 mN. The cutoff preload of the PPS-based USM was around 1800 mN, which was lower than that of the PPS/CF-based USM (2400 mN). The maximum angular velocity of the PEEK-based USM was around 20 rad/s and decreased to 0 with a preload of 500 mN. The variations in the optimal driving frequency

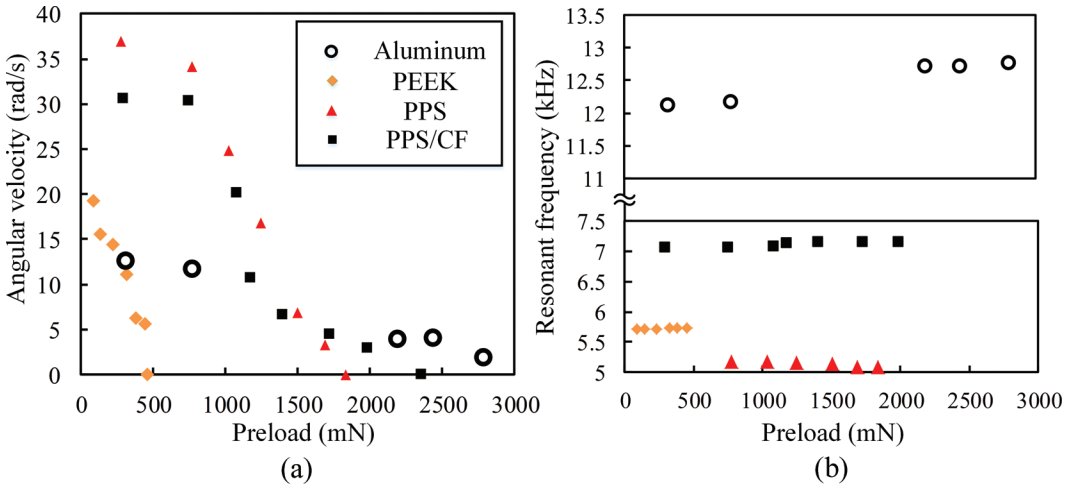

Fig. 10. Variation of angular velocities and optimal frequency of bimorphs as the preload increases.

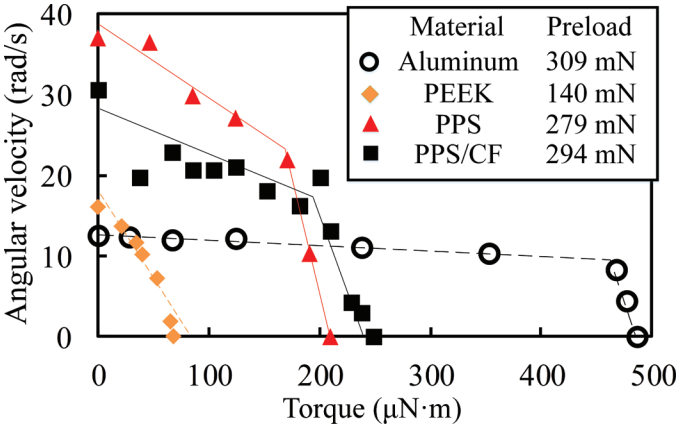

Fig. 11. Mechanical characteristics under a preload of less than 310 mN.

for the polymer-based USMs were smaller than 0.1 kHz before the USMs stopped. For the aluminum-based USM, angular velocity decreased from 11 to 5 rad/s when the preload was exerted to 2500 mN. Even though the driving frequency varied by more than 0.6 kHz, the rotor continued to rotate when the preload exceeded 2800 mN.

Next, we measured the mechanical characteristics of each USM under three different preload conditions. The experimental results are shown in Figs. 11, 12, and 13. The maximum angular velocity of the PPS-based USM was 36.9 rad/s for a preload of less than 310 mN. The rotor stopped rotating when the torque reached 210 μNm, as shown in Fig. 11. For the PPS/CF-based USM, the maximum angular velocity was approximately 30.5 rad/s, and the maximum torque reached 248 μNm. The angular velocities dropped suddenly at a certain torque in both the PPS- and the PPS/CF-based USMs. This implies that the friction force was insufficient because of the light preload. The aluminum-based USM also showed this feature; however, the maximum angular velocity was 12.5 rad/s, which was much lower than those of the PPS- and PPS/CF-based USMs. Maximum torque was approximately 500 μNm.

When the preload was increased to a medium range at around 770 mN, the maximum torques of the PPS-, PPS/CF-, and aluminum-based USMs all doubled under a 310-mN preload, as shown in Fig. 12, whereas the maximum angular velocities of the PPS- and PPS/CF-based USMs decreased to 34.1 and 30.3 rad/s, respectively. Mild drops in the velocity-torque characteristics were observed in the PPS- and PPS/CF-based USMs. Meanwhile, the PEEK-based USM was stopped under this preload.

When heavy preloads of over 2300 mN were applied, the PPS- and PPS/CF-based USMs stopped, whereas the aluminum-based USM continued to rotate although the speed was low, as shown in Fig. 13. The maximum torque measured for the aluminum-based USM was over 1800 μNm and a higher torque could also be loaded.

C. Discussion

To summarize our experimental results, there are the features of the polymer-based USMs: (1) polymer-based USMs have large angular velocities under light preload, (2) the maximum torque of a polymer-based USM is much lower than that of an aluminum-based USM because a large preload cannot be exerted on the polymer-based vibrator, and (3) among the tested materials, PPS is considered to be the suitable for vibrators of USMs under light preloads.

As discussed in previous studies [23], the rotation velocity of a USM is mainly determined by the vibration velocity of the stator. In the previous section, we explained the reason for high-vibration velocities in polymer vibrators. However, the rotation velocity of a polymer-based USM decreases rapidly as the preload increases. To consider this phenomenon, we measured the vibration velocities in the preloading direction (y-axis) and the tangential direction (z-axis) while the preload was increasing. Figs. 14 and 15 show the velocity variations in the PPS and the aluminum-based vibrators.

As the preload increases to 1600 mN, the vibration velocity along the z-axis decreases from 1000 to 200 mm/s, whereas the vibration velocity along the y-axis decreases from approximately 600 mm/s to 0. The variation in the resonance frequency is 0.05 kHz. By contrast, the vibration velocities of the aluminum-based vibrator in both di-

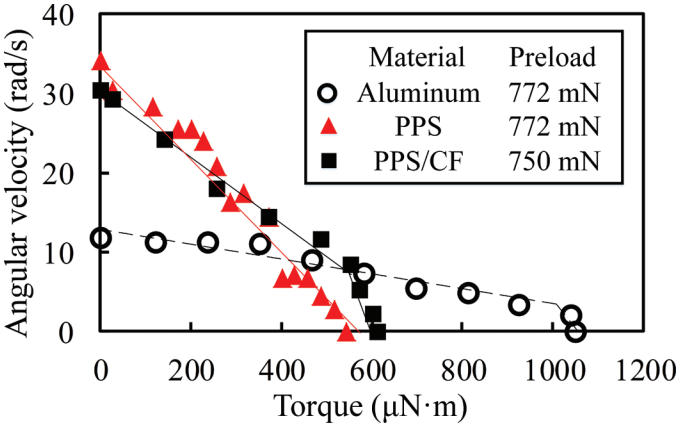

Fig. 12. Mechanical characteristics under a preload of around 770 mN.

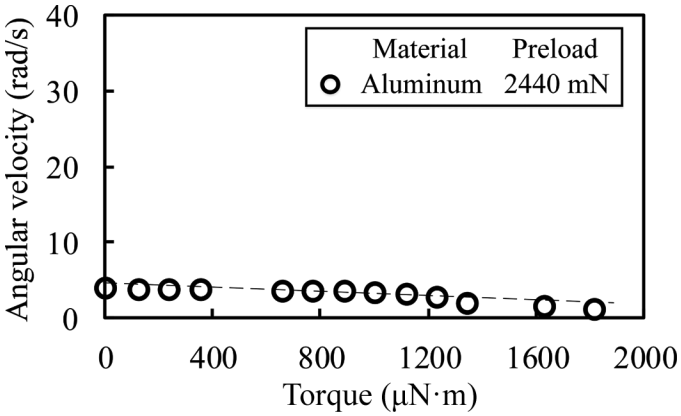

Fig. 13. Mechanical characteristics under a preload of 2440 mN.

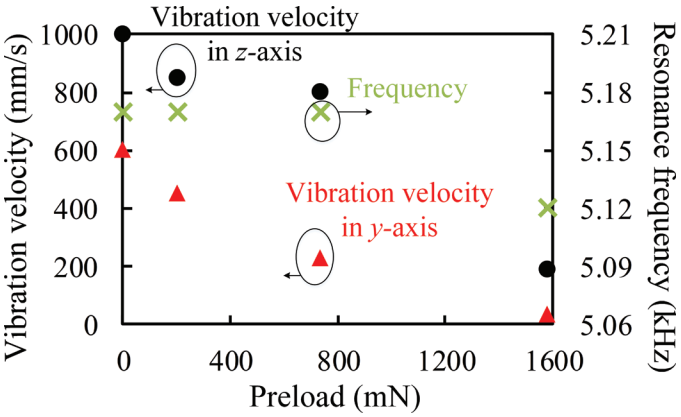

Fig. 14. Variation in the vibration velocities on the y-axis and z-axis and the resonance frequency of the PPS-based vibrator as the preload increases.

rections show little variation even with a large preload; however, the resonance frequencies of the vibrations in z-axis and y-axis are separating each other. The resonance frequencies along both z-axis and y-axis are the same without a preload, as summarized in Fig. 15. However, when the vibration velocity on the z-axis reaches its maximum value of 194 mm/s under a preload of 1.1 N, the velocity on the y-axis is only 10 mm/s. This implies that the orbit degenerates from an ellipse into a line, and motor operation becomes impossible. Although the driving frequency is set at 12.43 kHz, where the elliptical orbit can be maintained, the vibration velocity along the z-axis is insufficient to drive the rotor at this frequency. The shift in resonance frequency becomes larger and the angular velocity decreases further under a higher preload of 2.1 N.

In summary, for the polymer-based USM, the sharp decrease in the vibration velocity of the vibrator owing to increased preload leads to a decrease in the angular velocity of the rotor. For the aluminum-based USM, separation between the resonance frequencies of the vibrations in the preload direction and in the friction direction is the main cause of the decrease in the angular velocity of the rotor.

IV. Conclusions

To explore the feasibility of polymers in USMs, in this paper, PEEK, PPS, and PPS/CF were tested as vibrators of USMs. The polymer-based USMs worked successfully in the same way as conventional metal-based USMs, and their performances were compared with that of the aluminum-based USM. From our experiments, we reached the following conclusions:

1) Resonance frequencies of the polymer-based bimorphs are lower than that of the aluminum-based bimorph because of lower elastic modulus.
2) Vibration velocity of the polymer-based bimorph is higher than that of the aluminum-based bimorph because of lower elastic modulus.
3) The PPS-based bimorph has a higher vibration velocity than the other polymer-based bimorphs because it has a higher Q factor than the other polymers.
4) Polymer-based USMs have large angular velocities under light preloads, and the maximum torque of the polymer-based USM is lower than that of the aluminum-based USM because a large preload cannot be exerted on the polymer-based vibrator.
5) PPS is a suitable polymer for vibrators under light preloads, considering its vibration amplitude and light weight.
6) The sharp decrease in vibration velocity in the case of a polymer-based vibrator with a heavy preload leads to a decrease in angular velocity. Separation in the resonance frequencies of the vibrations in the preload direction and the friction direction in the

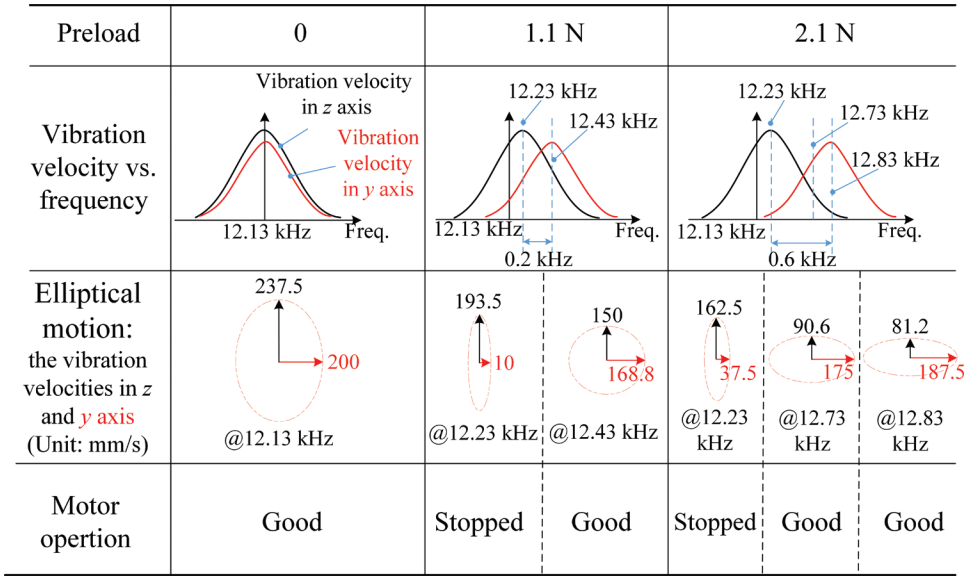

Fig. 15. Vibration velocity variations of the aluminum-based vibrator under increasing preloads and motor operation.

aluminum-based USM is the main cause of a decrease in the angular velocity of the rotor.

From these conclusions, we have a rough understanding of the feature of the polymer-based vibrators and USMs. However, all of the experiments were carried out at frequencies lower than the ultrasonic range. In the future, we will adjust the working frequency of the polymer-based motor to the ultrasonic range by decreasing its dimensions. The wear conditions on the contacting surface and the appropriate materials for the rotor are also worth investigating in future studies.

References

[1] K. Uchino, "Piezoelectric ultrasonic motors: Overview," *Smart Mater. Struct.*, vol. 7, no. 3, pp. 273–285, 1998.

[2] B. Watson, J. Friend, and L. Yeo, "Piezoelectric ultrasonic resonant motor with stator diameter less than 250 μm: The Proteus motor," *J. Micromech. Microeng.*, vol. 19, no. 2, art. no. 022001, 2009.

[3] T. Morita, M. K. Kurosawa, and T. Higuchi, "A cylindrical micro ultrasonic motor using PZT thin film deposited by single process hydrothermal method (Φ 2.4 mm, L = 10 mm stator transducer)," *IEEE Trans. Ultrason. Ferroelectr. Freq. Control*, vol. 45, no. 5, pp. 1178–1187, 1998.

[4] T. Morita, M. K. Kurosawa, and T. Higuchi, "A cylindrical shaped micro ultrasonic motor utilizing PZT thin film (1.4 mm in diameter and 5.0 mm long stator transducer)," *Sens. Actuators*, vol. 83, no. 1–3, pp. 225–230, 2000.

[5] T. Kanda, A. Makino, T. Ono, K. Suzumori, and M. K. Kurosawa, "A micro ultrasonic motor using a micro-machined bulk PZT transducer," *Sens. Actuators*, vol. 127, no. 1, pp. 131–138, 2006.

[6] H. Zhang, S. Dong, S. Zhang, T. Wang, Z. Zhang, and L. Fan, "Ultrasonic micro-motor using miniature piezoelectric tube with diameter of 1.0 mm," *Ultrasonics*, vol. 44, no. 22, pp. e603–e606, 2006.

[7] Y. Chen, K. Lu, T. Zhou, T. Liu, and C. Lu, "Study of a mini-ultrasonic motor with square metal bar and piezoelectric plate hybrid," *Jpn. J. Appl. Phys.*, vol. 45, no. 1, pp. 4780–4781, 2006.

[8] S. Manuspiya, P. Laoratanakul, and K. Uchino, "Integration of a piezoelectric transformer and an ultrasonic motor," *Ultrasonics*, vol. 41, no. 2, pp. 83–87, 2003.

[9] S. Dong, S.-P. Lim, K.-H. Lee, J. Zhang, L.-C. Lim, and K. Uchino, "Piezoelectric ultrasonic micromotor with 1.5 mm diameter," *IEEE Trans. Ultrason. Ferroelectr. Freq. Control*, vol. 50, no. 4, pp. 361–367, 2003.

[10] D. Yamagichi, T. Kanda, K. Suzumori, K. Fujisawa, K. Takegoshi, and T. Mizuno, "Ultrasonic motor using two sector-shaped piezoelectric transducers for sample spinning in high magnetic field," *J. Robot. Mechatron.*, vol. 25, no. 2, pp. 384–391, 2013.

[11] M. Takano, M. Takimoto, and K. Nakamura, "Electrode design of multilayer piezoelectric transducer for longitudinal-bending ultrasonic actuators," *Acoust. Sci. Technol.*, vol. 32, no. 3, pp. 100–108, 2011.

[12] D. P. Jones, D. C. Leach, and D. R. Moore, "Mechanical properties of poly(ether-ether-ketone) for engineering applications," *Polymer (Guildf.)*, vol. 26, no. 9, pp. 1385–1393, 1985.

[13] T. Ishii, S. Ueha, K. Nakamura, and K. Ohnishi, "Wear properties and life prediction of friction materials for ultrasonic motors," *Jpn. J. Appl. Phys.*, vol. 34, no. 1, pp. 2765–2770, 1995.

[14] J. Qu and T. Zhou, "An electric contact method to measure contact state between stator and rotor in a traveling wave ultrasonic motor," *Ultrasonics*, vol. 41, no. 7, pp. 561–567, 2003.

[15] P. Rehbein and J. Wallaschek, "Friction and wear behavior of polymer/steel and aluminum/alumina under high-frequency fretting conditions," *Wear*, vol. 216, no. 2, pp. 97–105, 1998.

[16] S. K. Sinha, S.-L. Thia, and L.-C. Lim, "A new tribometer for friction drives," *Wear*, vol. 262, no. 1–2, pp. 55–63, 2007.

[17] P. J. Rae, E. N. Brown, and E. B. Orler, "The mechanical properties of ploy(ether-ether-ketone) (PEEK) with emphasis on the large compressive strain response," *Polymer (Guildf.)*, vol. 48, no. 2, pp. 598–615, 2007.

[18] K. Nakamae, T. Nishino, Y. Shimizu, and K. Hata, "Temperature dependence of the elastic modulus of crystalline regions of polyoxymethylene," *Polymer (Guildf.)*, vol. 31, no. 10, pp. 1909–1918, 1990.

[19] S. R. Owen and J. F. Harper, "Mechanical, microscopical and fire retardant studies of ABS polymers," *Polym. Degrad. Stabil.*, vol. 64, no. 3, pp. 449–455, 1999.

[20] H. W. Hill and D. G. Brady, "Properties, environmental stability, and molding characteristics of polyphenylene sulfide," *Polym. Eng. Sci.*, vol. 16, no. 12, pp. 831–835, 1976.

[21] B. F. Ley, S. G. Lutz, and C. F. Rehberg, *Linear Circuit Analysis*. New York, NY, USA: McGraw-Hill Inc., 1959, pp. 278–279.

[22] K. F. Graff, *Wave Motion in Elastic Solids*. New York, NY, USA: Dover, 1991, pp. 155–158.

[23] K. Nakamura, M. Kurosawa, and S. Ueha, "Characteristics of a hybrid transducer-type ultrasonic motor," *IEEE Trans. Ultrason. Ferroelectr. Freq. Control*, vol. 38, no. 3, pp. 188–193, 1991.

Jiang Wu was born in Liaoning, China, on January 29, 1988. He received the B.E. degree in mechanical engineering from Dalian University of Technology (DUT), China, in 2010. From 2010 to 2012, he studied in the State Key Laboratory of Robotics and Systems, Harbin Institute of Technology (HIT), China, and received the M.E. degree in mechatronic engineering from HIT in 2012. He is currently a doctoral candidate in the Precision and Intelligence Laboratory, Tokyo Institute of Technology (TITECH), Japan. His research interests include piezoresistive and piezoelectric materials, permanent-magnet-based sensing technology, ultrasonic transducers and actuators, and ferroelectric film.

Yosuke Mizuno was born in Hyogo, Japan, on October 13, 1982. He received the B.E., M.E., and Dr.Eng. degrees in electronic engineering from the University of Tokyo, Japan, in 2005, 2007, and 2010, respectively.

From 2007 to 2010, he was engaged in Brillouin optical correlation-domain reflectometry for his Dr.Eng. degree at the University of Tokyo. From 2007 to 2010, he was a Research Fellow (DC1) of the Japan Society for the Promotion of Science (JSPS). From 2010 to 2012, as a Research Fellow (PD) of JSPS, he worked on polymer optics at Tokyo Institute of Technology, Japan. In 2011, he stayed at BAM Federal Institute for Materials Research and Testing, Germany, as a Visiting Research Associate. Since 2012, he has been an Assistant Professor at the Precision and Intelligence Laboratory, Tokyo Institute of Technology, where he is active in fiber-optic sensing, polymer optics, and ultrasonics.

Dr. Mizuno is the winner of the Funai Research Award 2010, the Ando Incentive Prize for the Study of Electronics 2011, the NF Foundation R&D Encouragement Award 2012, and the Challenging Research Award 2013. He is a member of the IEEE, the Japanese Society of Applied Physics (JSAP), and the Institute of Electronics, Information, and Communication Engineers (IEICE) of Japan.

Marie Tabaru was born in Tokyo, Japan. She received her B.Eng. degree in electrical and electronic engineering from the Tokyo Institute of Technology in 2002 and her M.E. degree in human system science in 2005. She studied image signal processing of medical ultrasound at the University of Washington, Seattle, from 2002 to 2003. She received the Best Student Paper Award in Engineering Acoustics from the Acoustical Society of America in 2006. She received her D.E. degree from the Tokyo Institute of Technology in 2007. She has been an associate professor of the Precision and Intelligence Laboratory, Tokyo Institute of Technology, since 2013. She is a member of the Acoustical Society of Japan, the Japan Society of Ultrasonics in Medicine, and the Institute of Electronics, Information and Communication Engineers.

Kentaro Nakamura was born in Tokyo, Japan, on July 3, 1963. He received the B.E., M.E., and Dr.Eng. degrees from the Tokyo Institute of Technology, Japan, in 1987, 1989, and 1992, respectively.

Since 2010, he has been a Professor at the Precision and Intelligence Laboratory, Tokyo Institute of Technology. His research field is the applications of ultrasonic waves, measurement of vibration and sound using optical methods, and fiber-optic sensing.

Prof. Nakamura is the winner of the Awaya Kiyoshi Award for encouragement of research from the Acoustical Society of Japan (ASJ) in 1996, and the Best Paper Awards from the Institute of Electronics, Information and Communication Engineers (IEICE) in 1998 and from the Symposium on Ultrasonic Electronics (USE) in 2007 and 2011. He also received the Japanese Journal of Applied Physics (JJAP) Editorial Contribution Award from the Japan Society of Applied Physics (JSAP) in 2007. He is a member of the IEEE, the ASJ, the JSAP, the IEICE, and the Institute of Electrical Engineers of Japan (IEEJ).